

Angle-based Localization and Rigidity Maintenance Control for Multi-Robot Networks

J. Francisco Presenza^{* 1}, Leonardo J. Colombo², Juan I. Giribet³, and Ignacio Mas³

¹Institute of Engineering Technology and Sciences “Hilario Fernández Long” (CONICET-UBA) - Av. Paseo Colón 850, C1063ACV, Buenos Aires, Argentina.

²Centre for Automation and Robotics (CSIC-UPM) - Ctra. M300 Campo Real, Km 0.200, Arganda del Rey, 28500, Madrid, Spain.

³Artificial Intelligence and Robotics Laboratory (UDES) and CONICET - Vito Dumas 284, B1644BID, Victoria, Argentina.

Abstract

In this work, we study angle-based localization and rigidity maintenance control for multi-robot networks under sensing constraints. We establish the first equivalence between angle rigidity and bearing rigidity considering *directed* sensing graphs and *body-frame* bearing measurements in both 2 and 3-dimensional space. In particular, we demonstrate that a framework in $SE(d)$ is infinitesimally bearing rigid if and only if it is infinitesimally angle rigid and each robot obtains at least $d - 1$ bearing measurements ($d \in \{2, 3\}$). Building on these findings, this paper proposes a distributed angle-based localization scheme and establishes local exponential stability under switching sensing graphs, requiring only infinitesimal angle rigidity across the visited topologies. Then, since angle rigidity strongly depends on the robots’ spatial configuration, we investigate rigidity maintenance control. The *angle rigidity eigenvalue* is presented as a metric for the degree of rigidity. A decentralized gradient-based controller capable of executing mission-specific commands while maintaining a sufficient level of angle rigidity is proposed. Simulations were conducted to evaluate the scheme’s effectiveness and practicality.

1 Introduction

Cooperative localization is a fundamental problem in multi-robot systems, enabling the decentralized estimation of robot positions and orientations using only inter-agent measurements. Over the past decade, extensive research has focused on *bearing-based* methods, which exploit line-of-sight direction measurements between robots. Recently, *angle-based* approaches, which employ the angles between pairs of measured bearings,

have emerged as a particularly attractive alternative. *Rigidity theory* studies whether the available measurements (bearings or angles) are sufficient to infer the robots’ positions and, depending on the context, the orientations as well.

Early approaches to bearing-based localization commonly assumed that all measurements were expressed in a common reference frame, implying that each agent knows its orientation. This allows for the modeling of the robot states as elements of \mathbb{R}^d and the use of undirected sensing networks, since the two bearings corresponding to a pair of robots carry the same information. Such a setup resulted in protocols with global convergence guarantees under mild conditions, e.g., containing a spanning Laman subgraph; see [32] and references therein. However, this assumption can be hard to meet in practice since the sensors used for absolute orientation estimation, such as compasses, are either unavailable or strongly affected by magnetic disturbances. Additionally, due to sensor limitations, such as narrow camera fields of view, bearing measurements are generally not bidirectional; that is, robot i may observe robot j , but not vice versa. For these reasons, real-world multi-robot systems must handle unknown robot poses in $SE(d)$, along with directed sensing graphs.

Following this, many works have proposed exploiting the body-frame bearing measurements for orientation estimation; see [21, 31, 24, 29, 16, 27, 4, 2] and references therein. For example, [21] restricts the robot poses to $SE(2)$ and considers that all bearing measurements are bidirectional—rendering an undirected sensing graph. Under these conditions, orientations can be estimated from bearings, provided that the graph is connected. In $SE(3)$, bidirectional bearings and graph connectivity are not sufficient; hence, [29, 16, 27, 4, 2] require more involved sensing topologies, e.g., some pairs of robots with bidirectional bearings and common neighbors. Other schemes consider directed graphs under the more general condition of infinitesimal bearing rigidity, but these approaches are restricted to $SE(2)$ [31] and $\mathbb{R}^3 \times \mathbb{S}^1$ [24]. The primary limitation of all these approaches arises from the constraints associated with

^{*}This work was partially supported by Universidad de Buenos Aires [grant number UBACyT 20020220100053BA]. L. Colombo acknowledge financial support from Grant PID2022-137909NB-C21 funded by MCIN/AEI/ 10.13039/501100011033 and iRoboCity2030-CM, Robótica Inteligente para Ciudades Sostenibles (TEC-2024/TEC-62). Corresponding author J. Francisco Presenza.

estimating orientations from bearings. Indeed, they require at least $d - 1$ outgoing neighbors per robot, constraining the robots' freedom of motion, as all cameras must be engaged in mutual sensing.

Subsequent strategies assumed the availability of relative orientation measurements to estimate all orientations in a common frame [28, 17, 3]. Once the orientations are recovered, common-frame bearing-based localization can be implemented to estimate the robots positions with global convergence guarantees. While an appealing alternative, this approach introduces an extra layer of complexity since the estimation must be performed on the manifold $\text{SE}(d)$ and because orientation measurement noise propagates into the position estimates.

More recently, motivated by these challenges, several works have focused on angle-based localization; see [11, 6, 8, 7]. These angles are independent of the reference frame; hence, orientation estimation procedures can be avoided, simplifying the description and reducing the system's dimensionality. As a consequence, angle-based localization does not require a minimum number of bearing measurements per robot (some robots might not acquire bearing measurements at all), thus increasing their freedom of motion. Although existing work provides solid theoretical foundations, several shortcomings prevent their use in real-world applications. For example, the localization schemes found in [11, 6, 8, 7] are only applicable in \mathbb{R}^2 or require special topologies such as triangular and tetrahedral in \mathbb{R}^2 and \mathbb{R}^3 , respectively. Developing localization schemes that allow for arbitrary directed and time-varying topologies can significantly improve the applicability of these systems.

Despite the close connection between bearing-based and angle-based coordination, their relationship remains poorly understood, except under restrictive assumptions. For example, recent works have established the equivalence between bearing rigidity and angle rigidity [12] or signed angle rigidity [10] but only in \mathbb{R}^2 . Additionally, these findings assume that all bearings are measured in a common frame, constraining the analysis to undirected graphs. In contrast, the results developed in this paper consider *directed* sensing graphs and *body-frame* bearing measurements in both 2 and 3-dimensional space. In particular, as our first main contribution, we show that in $\text{SE}(d)$ ($d \in \{2, 3\}$), infinitesimal bearing rigidity holds if and only if the framework is infinitesimally angle rigid and each robot obtains at least $d - 1$ bearing measurements. To our knowledge, this is the first formal equivalence between bearing rigidity and angle rigidity that naturally applies to vision-based multi-robot systems since it (a) does not require bidirectional bearing measurements; (b) deals with body-frame measurements; and (c) works beyond the plane. In addition, as our second main contribution, we propose a distributed angle-based localization scheme, and establish local exponential stability under directed switching topologies provided that all visited graphs are infinitesimally angle rigid.

Finally, we study the design of control schemes

that enable robots to follow arbitrary trajectories while guaranteeing the required observability conditions. This problem, which is an important aspect of cooperative localization, has been studied in [5] and [9] employing nonlinear observability methods for the cases of bearing and distance measurements, respectively. However, such methods do not account for changes in the sensing topology, which is inherently dynamic due to robot motion. In contrast, rigidity—a first-order approximation of nonlinear observability—has been studied for time-varying networks in [30, 23] for distances and in [25, 22] for bearings. In this work, and as our third main contribution, we extend these techniques to the case of angle measurements. We present the angle rigidity eigenvalue and propose its use as a metric for the degree of rigidity. A decentralized gradient-based controller capable of executing mission-specific commands while maintaining a sufficient level of rigidity is proposed. The controller preserves angle rigidity by keeping the rigidity eigenvalues above a threshold. To validate the proposed approach, a mission involving multiple target tracking is proposed, which produces changes in the sensing topology that challenge the rigidity condition and test the capabilities of the controller. Simulations were performed to evaluate the effectiveness of the scheme.

The remainder of this paper is organized as follows. Section 2 presents basic definitions and an overview of the bearing and angle rigidity theory in $\text{SE}(d)$. Section 3 establishes the equivalence between bearing rigidity and angle rigidity. The angle-based position estimator and the rigidity maintenance controller are introduced in Section 4, together with a discussion of their convergence and decentralized implementation. The simulation results are presented in Section 5, and Section 6 provides final conclusions and directions for future work.

2 Preliminaries and Notation

Lowercase letters without a superscript, e.g., $x \in \mathbb{R}^d$ are used to express a vector in a common reference frame associated with the standard basis $\{e_1, \dots, e_d\} \subset \mathbb{R}^d$. A column stack of n vectors v_1, \dots, v_n is represented as $[v_1; \dots; v_n]$ and also as $[v_i]_{i \in \mathcal{I}}$ given $\mathcal{I} = \{1, \dots, n\}$. The vector of all zeros and all ones are $\mathbf{0}_n, \mathbf{1}_n \in \mathbb{R}^n$, respectively, and the identity matrix is $\mathbf{I}_n \in \mathbb{R}^{n \times n}$. The null space of a matrix is $\text{Null}(A)$, and the Kronecker product is symbolized as $A \otimes B$. The unit d -sphere is $\mathbb{S}^{d-1} = \{v \in \mathbb{R}^d : \|v\| = 1\}$.

Let \mathcal{M} be a smooth manifold, then the tangent and normal spaces at $x \in \mathcal{M}$ are denoted as $T_x\mathcal{M}$ and $N_x\mathcal{M}$, respectively. The gradient at x of a differentiable scalar-valued function $f : \mathcal{M} \rightarrow \mathbb{R}$ is defined as the unique element of $T_x\mathcal{M}$ that satisfies

$$\langle \nabla_x f(x), v \rangle = (d_x f)(v), \quad \forall v \in T_x\mathcal{M},$$

where $d_x f$ is the differential of f at x and $\langle \cdot, \cdot \rangle$ denotes a Riemannian metric on \mathcal{M} . For more details, see [15].

Let $\text{SE}(d) = \mathbb{R}^d \times \text{SO}(d)$ be the special Euclidean group. Here $\text{SO}(d)$ corresponds to the Lie group of ro-

tation matrices, and its Lie algebra $\mathfrak{so}(d)$ denotes the space of skew-symmetric matrices, both of dimension $d' := \binom{d}{2}$. Now, let $S : \mathbb{R}^{d'} \rightarrow \mathfrak{so}(d)$ be the invertible linear map such that for all $x \in \mathbb{R}^{d'}$ and $y \in \mathbb{R}^d$, $S(x)y = x[-y_2; y_1]$ when $d = 2$, and $S(x)y = x \times y$ when $d = 3$. Let $\omega \in \mathbb{R}^{d'}$ denote an angular velocity. Then the time derivative of the rotation matrix R satisfies $\dot{R} = S(\omega)R$.

In this work, the sensing network is modeled by a directed graph denoted as $\mathcal{G} = (\mathcal{V}, \mathcal{E})$ with a vertex set $\mathcal{V} = \{1, \dots, N\}$ and an edge set $\mathcal{E} \subseteq \mathcal{V} \times \mathcal{V}$. Here, $(i, j) \in \mathcal{E}$ means that agent i detects agent j with its bearing sensor. The use of directed graphs allows us to account for the non-reciprocity of the bearing measurements. The set of (outgoing) neighbors of i is $\mathcal{O}_i = \{j : (i, j) \in \mathcal{E}\}$. Let (p_i, R_i) represent the pose of robot i , with position $p_i \in \mathbb{R}^d$ and orientation $R_i \in \text{SO}(d)$; and (\mathbf{p}, \mathbf{R}) with $\mathbf{p} = [p_i]_{i \in \mathcal{V}} \in \mathbb{R}^{d|\mathcal{V}|}$ and $\mathbf{R} = [R_i]_{i \in \mathcal{V}} \in \text{SO}(d)^{|\mathcal{V}|}$ represents the joint configuration. A *framework* is a pair consisting of a graph and a joint pose. Depending on the context, it may be written as $(\mathcal{G}, (\mathbf{p}, \mathbf{R}))$ when orientations are included, or as $(\mathcal{G}, \mathbf{p})$ when only positions are considered.

The body-frame bearing acquired when $j \in \mathcal{O}_i$ is described by the unit vector $\beta_{ij}^i := R_i^\top \beta_{ij}$ where $\beta_{ij} := p_{ij}/d_{ij}$, $p_{ij} := p_j - p_i$, and $d_{ij} := \|p_{ij}\|$. Throughout this work, we assume that $p_i \neq p_j$ for all $i, j \in \mathcal{V}$. The (cosine of the) angle measurement obtained when $\{j, k\} \subseteq \mathcal{O}_i$ is $\alpha_{ijk} := \beta_{ij}^\top \beta_{ik} = (\beta_{ij}^i)^\top \beta_{ik}^i$. The set of all angle indices is $\mathcal{A} := \{(i, j, k) : \{j, k\} \subseteq \mathcal{O}_i, j < k\}$. Note that we define \mathcal{A} to include all angles induced by a given edge set \mathcal{E} , as this is the most natural way to represent observed angles.

2.1 Bearing Rigidity

Bearing rigidity in $\text{SE}(d)$ studies the conditions under which robot poses can be reconstructed from body-frame bearing measurements up to a similarity transformation; that is, any combination of uniform translations, rotations, reflections, and scalings.

Consider a framework $(\mathcal{G}, (\mathbf{p}, \mathbf{R}))$ over $\text{SE}(d)$, $d \in \{2, 3\}$. Let $\beta_{\mathcal{G}} : (\text{SE}(d))^{|\mathcal{V}|} \rightarrow (\mathbb{S}^{d-1})^{|\mathcal{E}|}$ be such that $\beta_{\mathcal{G}}(\mathbf{p}, \mathbf{R}) = (\beta_{ij}^i)_{(i,j) \in \mathcal{E}}$ is denoted as the *bearing function*. The *bearing rigidity matrix* $B_{\mathcal{G}}(\mathbf{p}, \mathbf{R}) \in \mathbb{R}^{d|\mathcal{E}| \times (d+d')|\mathcal{V}|}$ is the differential of $\beta_{\mathcal{G}}$, which maps robot linear and angular velocities to bearing velocities,

$$\dot{\beta}_{\mathcal{G}} = B_{\mathcal{G}}(\mathbf{p}, \mathbf{R}) \begin{bmatrix} \mathbf{v} \\ \boldsymbol{\omega} \end{bmatrix},$$

where $\mathbf{v} = [v_i]_{i \in \mathcal{V}} \in \mathbb{R}^{d|\mathcal{V}|}$ and $\boldsymbol{\omega} = [\omega_i]_{i \in \mathcal{V}} \in \mathbb{R}^{d'|\mathcal{V}|}$. It is useful to make the structure of the rigidity matrix explicit. To this end, let $B_{ij}(\mathbf{p}, \mathbf{R})$ be the $d \times d|\mathcal{V}|$ block row corresponding to the edge $(i, j) \in \mathcal{E}$. It follows that

$$\dot{\beta}_{ij}^i = B_{ij}(\mathbf{p}, \mathbf{R}) \begin{bmatrix} \mathbf{v} \\ \boldsymbol{\omega} \end{bmatrix} = R_i^\top \left(\frac{P_{ij}}{d_{ij}} (v_j - v_i) - S(\omega_i) \beta_{ij} \right), \quad (1)$$

where $P_{ij} := \mathbf{I}_d - \beta_{ij} \beta_{ij}^\top$ is the orthogonal projection matrix onto $\text{span}\{\beta_{ij}\}^\perp$. We will also use this matrix in the robot's i reference frame, i.e., $P_{ij}^i := \mathbf{I}_d - \beta_{ij}^i (\beta_{ij}^i)^\top$.

Consider an infinitesimal motion of (\mathbf{p}, \mathbf{R}) generated by a similarity transformation. The space of all such motions is

$$\mathcal{T}_b(\mathbf{p}, \mathbf{R}) = \{[\mathbf{v}; \boldsymbol{\omega}] : v_i = \kappa p_i + S(\omega)p_i + v, \omega_i = \omega, \kappa \in \mathbb{R}, \omega \in \mathbb{R}^{d'}, v \in \mathbb{R}^d, \forall i \in \mathcal{V}\}. \quad (2)$$

It follows that $\dim \mathcal{T}_b(\mathbf{p}, \mathbf{R}) = d + d' + 1$ and $\mathcal{T}_b(\mathbf{p}, \mathbf{R}) \subseteq \text{Null } B_{\mathcal{G}}(\mathbf{p}, \mathbf{R})$; see [19]. We are now ready to define infinitesimal bearing rigidity in $\text{SE}(d)$.

Definition 1 A framework $(\mathcal{G}, (\mathbf{p}, \mathbf{R}))$ is said to be *infinitesimally bearing rigid (IBR)* if

$$\text{Null } B_{\mathcal{G}}(\mathbf{p}, \mathbf{R}) = \mathcal{T}_b(\mathbf{p}, \mathbf{R}).$$

Equivalently, if $\text{rank } B_{\mathcal{G}}(\mathbf{p}, \mathbf{R}) = (d+d')|\mathcal{V}| - (d+d'+1)$.

Infinitesimal bearing rigidity allows for the local recovery of the true poses up to a similarity transformation. This is formalized by the following proposition, which follows directly from [20, Theorem 4].

Proposition 1 Let $(\mathcal{G}, (\mathbf{p}, \mathbf{R}))$ be an infinitesimally bearing rigid framework. Then, there exists an open neighborhood \mathcal{U} of (\mathbf{p}, \mathbf{R}) such that if $(\mathbf{q}, \mathbf{Q}) \in \mathcal{U}$ and $\beta_{\mathcal{G}}(\mathbf{p}, \mathbf{R}) = \beta_{\mathcal{G}}(\mathbf{q}, \mathbf{Q})$ then (\mathbf{p}, \mathbf{R}) and (\mathbf{q}, \mathbf{Q}) are related by a similarity transformation.

2.2 Angle Rigidity

Angle rigidity studies the conditions under which robot positions can be reconstructed from angle measurements, up to a similarity transformation. Angle measurements are independent of the robots' body frames; hence, the robots can be modeled as $\mathbf{p} \in \mathbb{R}^{d|\mathcal{V}|}$. Some approaches, such as [7], incorporate a common reference direction (e.g., gravity), which provides additional information and can relax the requirements on the sensing topology. In this work, however, we assume no prior knowledge of the robots' orientations, as this corresponds to the most general setting.

Consider a framework $(\mathcal{G}, \mathbf{p})$ and let \mathcal{A} be the set of angle indices induced by \mathcal{E} . Let $\boldsymbol{\alpha}_{\mathcal{G}} : \mathbb{R}^{d|\mathcal{V}|} \rightarrow \mathbb{R}^{|\mathcal{A}|}$ such that $\boldsymbol{\alpha}_{\mathcal{G}}(\mathbf{p}) = (\alpha_{ijk})_{(i,j,k) \in \mathcal{A}}$ be the *angle function*, and let the *angle rigidity matrix* $A_{\mathcal{G}}(\mathbf{p}) \in \mathbb{R}^{|\mathcal{A}| \times d|\mathcal{V}|}$ be the differential of $\boldsymbol{\alpha}_{\mathcal{G}}$. The latter relates tangent vectors, i.e., $\dot{\boldsymbol{\alpha}}_{\mathcal{G}} = A_{\mathcal{G}}(\mathbf{p})\mathbf{v}$, where $\mathbf{v} = [v_i]_{i \in \mathcal{V}} \in \mathbb{R}^{d|\mathcal{V}|}$. To make the structure of the rigidity matrix explicit, consider $A_{ijk}(\mathbf{p}) \in \mathbb{R}^{1 \times d|\mathcal{V}|}$, i.e., the row corresponding to $(i, j, k) \in \mathcal{A}$. Then,

$$\dot{\alpha}_{ijk} = A_{ijk}(\mathbf{p})\mathbf{v} = \beta_{ik}^\top \frac{P_{ij}}{d_{ij}} (v_j - v_i) + \beta_{ij}^\top \frac{P_{ik}}{d_{ik}} (v_k - v_i). \quad (3)$$

In the angle case, the space of infinitesimal motions induced by similarity transformations is

$$\mathcal{T}_a(\mathbf{p}) = \{\mathbf{v} : v_i = \kappa p_i + S(\omega)p_i + v, \kappa \in \mathbb{R}, \omega \in \mathbb{R}^{d'}, v \in \mathbb{R}^d, \forall i \in \mathcal{V}\}. \quad (4)$$

It follows that $\dim \mathcal{T}_a(\mathbf{p}) = d + d' + 1$ and $\mathcal{T}_a(\mathbf{p}) \subseteq \text{Null } A_{\mathcal{G}}(\mathbf{p})$. We define infinitesimal angle rigidity as follows.

Definition 2 A framework $(\mathcal{G}, \mathbf{p})$ in \mathbb{R}^d is said to be infinitesimally angle rigid (IAR) if

$$\text{Null } A_{\mathcal{G}}(\mathbf{p}) = \mathcal{T}_a(\mathbf{p}).$$

Equivalently, if $\text{rank } A_{\mathcal{G}}(\mathbf{p}) = d|\mathcal{V}| - (d + d' + 1)$.

Infinitesimal angle rigidity enables the local recovery of the true positions up to a similarity transformation.

Proposition 2 ([12, Theorem 2]) Let $(\mathcal{G}, \mathbf{p})$ be an infinitesimally angle rigid framework. Then, there exists an open neighborhood \mathcal{U} of \mathbf{p} such that if $\mathbf{q} \in \mathcal{U}$ and $\alpha_{\mathcal{G}}(\mathbf{p}) = \alpha_{\mathcal{G}}(\mathbf{q})$ then \mathbf{p} and \mathbf{q} are related by a similarity transformation.

3 Relation between Angle and Bearing Rigidity

In this section, we present the formal relationship between bearing rigidity and angle rigidity for arbitrary directed graphs in $\text{SE}(d)$.

Definition 3 A framework $(\mathcal{G}, \mathbf{p})$ in $\mathbb{R}^{d|\mathcal{V}|}$ is said to be degenerate if there exists $i \in \mathcal{V}$, such that $|\mathcal{O}_i| \geq d$ and $\dim \mathcal{B}_i \leq d - 1$, where $\mathcal{B}_i := \text{span}\{\beta_{ij} : j \in \mathcal{O}_i\} \subseteq \mathbb{R}^d$.

Definition 3 characterizes a framework as degenerate if it includes at least one vertex that has enough outgoing bearings to span \mathbb{R}^d , yet those bearings are contained in a proper subspace. Fig. 1 illustrates this condition. It can be checked that the frameworks in Figs. 1a and 1c are infinitesimally bearing rigid but not infinitesimally angle rigid. On the other hand, the frameworks in Figs. 1b and 1d are both infinitesimally bearing rigid and infinitesimally angle rigid. Degeneracy is relevant to our purposes since, for degenerate frameworks, the equivalence between bearing rigidity and angle rigidity presented in Theorem 1 does not hold. However, as shown in Proposition 3, the non-degeneracy condition holds for almost all configurations $\mathbf{p} \in \mathbb{R}^{d|\mathcal{V}|}$ (Lebesgue-a.e.).

Proposition 3 Let $\mathcal{G} = (\mathcal{V}, \mathcal{E})$ be a directed graph and let $d \geq 2$. Consider the set of degenerate configurations

$$\mathcal{D}(\mathcal{G}) := \{\mathbf{p} \in \mathbb{R}^{d|\mathcal{V}|} : (\mathcal{G}, \mathbf{p}) \text{ is degenerate}\}.$$

Then \mathcal{D} is contained in a finite union of proper algebraic varieties in $\mathbb{R}^{d|\mathcal{V}|}$. In particular, \mathcal{D} has Lebesgue measure zero. Consequently, non-degenerate configurations are generic in both \mathbb{R}^2 and \mathbb{R}^3 .

Proof. Fix $i \in \mathcal{V}$ and assume $|\mathcal{O}_i| \geq d$. From Definition 3 and since the linear span does not change under nonzero scalar normalization, it follows that $\mathcal{B}_i = \text{span}\{p_{ij} : j \in \mathcal{O}_i\}$. Therefore, $\dim \mathcal{B}_i \leq d - 1$ is equivalent to saying that the family $\{p_{ij}\}_{j \in \mathcal{O}_i}$ is linearly dependent. Equivalently, for every d -tuple $J = \{j_1, \dots, j_d\} \subseteq \mathcal{O}_i$, it holds that

$$\det M_{i,J}(\mathbf{p}) = 0, \quad M_{i,J}(\mathbf{p}) := [p_{ij_1} \ \dots \ p_{ij_d}] \in \mathbb{R}^{d \times d}.$$

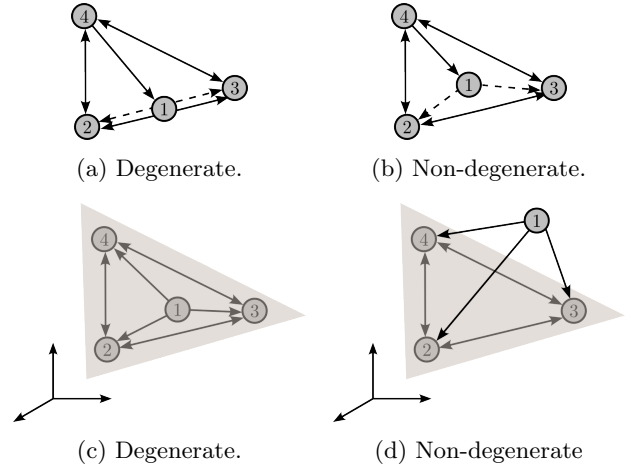


Figure 1: Configuration degeneracy: (a) and (c) degenerate configurations in \mathbb{R}^2 and \mathbb{R}^3 due to collinearity and coplanarity between $\{1, 2, 3\}$ and $\{1, 2, 3, 4\}$, respectively; (b) and (d) breaking collinearity (coplanarity) removes degeneracy.

Now define, for each pair (i, J) with $i \in \mathcal{V}$ and $J \subseteq \mathcal{O}_i$, $|J| = d$, the set

$$\mathcal{Z}_{i,J} := \{\mathbf{p} \in \mathbb{R}^{d|\mathcal{V}|} : \det M_{i,J}(\mathbf{p}) = 0\}.$$

Hence, for each fixed i we obtain the characterization

$$\{\mathbf{p} : \dim \mathcal{B}_i \leq d - 1\} = \bigcap_{\substack{J \subseteq \mathcal{O}_i \\ |J|=d}} \mathcal{Z}_{i,J}. \quad (5)$$

Observe that $\det M_{i,J}(\mathbf{p})$ is a polynomial in the coordinates of \mathbf{p} : each entry of $M_{i,J}(\mathbf{p})$ is affine in $(p_i, p_{j_1}, \dots, p_{j_d})$, and the determinant is a multilinear polynomial in the entries. Therefore $\mathcal{Z}_{i,J}$ is an algebraic variety.

We next show that $\mathcal{Z}_{i,J}$ is proper, i.e., $\det M_{i,J}$ is not the zero polynomial. Indeed, fix any i and $J = \{j_1, \dots, j_d\}$. Choose a configuration $\bar{\mathbf{p}}$ such that

$$\bar{p}_i = 0, \quad \bar{p}_{j_k} = e_k, \quad k = 1, \dots, d,$$

where $\{e_1, \dots, e_d\}$ is the standard basis of \mathbb{R}^d . Then $M_{i,J}(\bar{\mathbf{p}}) = \mathbf{I}_d$, so $\det M_{i,J}(\bar{\mathbf{p}}) \neq 0$. Thus, $\det M_{i,J}$ is not the zero polynomial. It is well known from standard measure theory that the zero set of a nonzero polynomial in \mathbb{R}^n , in our case $\mathcal{Z}_{i,J} \subset \mathbb{R}^{d|\mathcal{V}|}$, has Lebesgue measure zero.

Finally, by Definition 3 and (5),

$$\mathcal{D} = \bigcup_{\substack{i \in \mathcal{V} \\ |\mathcal{O}_i| \geq d}} \{\mathbf{p} : \dim \mathcal{B}_i \leq d - 1\} = \bigcup_{\substack{i \in \mathcal{V} \\ |\mathcal{O}_i| \geq d}} \bigcap_{\substack{J \subseteq \mathcal{O}_i \\ |J|=d}} \mathcal{Z}_{i,J}.$$

A finite union of measure-zero sets has measure zero, and therefore \mathcal{D} has Lebesgue measure zero. This proves the claim. \square

Now we present the main result of Section 3. This result shows that angle-based multi-robot coordination is more advantageous than bearing-based coordination, because the set of IAR frameworks strictly contains the

set of IBR frameworks. In practice, using angles allows some robots to dedicate their sensors to useful tasks, such as monitoring the environment instead of engaging in mutual observation at all times.

Theorem 1 *Let $d \in \{2, 3\}$ and let $(\mathcal{G}, (\mathbf{p}, \mathbf{R}))$ be a framework in $\text{SE}(d)$ such that $(\mathcal{G}, \mathbf{p})$ is non-degenerate. Then, $(\mathcal{G}, (\mathbf{p}, \mathbf{R}))$ is infinitesimally bearing rigid if and only if $(\mathcal{G}, \mathbf{p})$ is infinitesimally angle rigid and $\dim \mathcal{B}_i \geq d - 1$, for all $i \in \mathcal{V}$.*

Proof. For convenience, we will focus on the case $d = 3$; the case $d = 2$ follows analogously.

Sufficiency: We proceed by the contrapositive, which leads us to two cases.

First, assume that $\dim \mathcal{B}_{i^*} \leq d - 2 = 1$ for some $i^* \in \mathcal{V}$. On one hand, if $\mathcal{B}_{i^*} = \{\mathbf{0}_d\}$ then $(\mathcal{G}, (\mathbf{p}, \mathbf{R}))$ cannot be IBR, because $\beta_{\mathcal{G}}$ would be invariant under changes in R_{i^*} . On the other hand, consider $\dim(\mathcal{B}_{i^*}) = 1$. Define $\bar{\omega} = [\bar{\omega}_i]_{i \in \mathcal{V}} \in \mathbb{R}^{3|\mathcal{V}|}$ such that $\bar{\omega}_i = 0$ for all $i \in \mathcal{V} \setminus \{i^*\}$ and $\bar{\omega}_{i^*} = \beta_{i^* j^*}$ for some $j^* \in \mathcal{O}_{i^*}$. It follows that $S(\bar{\omega}_{i^*})\beta_{i^* j^*} = 0$ for all $j^* \in \mathcal{O}_{i^*}$. Let $\bar{\mathbf{v}} = \mathbf{0} \in \mathbb{R}^{3|\mathcal{V}|}$. Then $[\bar{\mathbf{v}}; \bar{\omega}] \notin \mathcal{T}_b(\mathbf{p}, \mathbf{R})$ and $B_{\mathcal{G}}(\mathbf{p}, \mathbf{R})[\bar{\mathbf{v}}; \bar{\omega}] = 0$ (see (1)); hence, the framework is not IBR.

Second, consider $(\mathcal{G}, \mathbf{p})$ that is not IAR for which $\dim(\mathcal{B}_i) \geq d - 1 = 2$ for each $i \in \mathcal{V}$. The first condition means that we can pick $\bar{\mathbf{v}} \notin \mathcal{T}_a(\mathbf{p})$ such that $A_{\mathcal{G}}(\mathbf{p})\bar{\mathbf{v}} = 0$. Our goal is to show that, irrespective of the choice of $\mathbf{R} \in \text{SE}(d)^{|\mathcal{V}|}$, the framework $(\mathcal{G}, (\mathbf{p}, \mathbf{R}))$ is not IBR. To do that, we will construct $\bar{\omega}$ such that $[\bar{\mathbf{v}}; \bar{\omega}] \notin \mathcal{T}_b(\mathbf{p}, \mathbf{R})$ and $B_{\mathcal{G}}(\mathbf{p}, \mathbf{R})[\bar{\mathbf{v}}; \bar{\omega}] = 0$. The latter equates to (see (1))

$$S(\beta_{i\nu})\bar{\omega}_i = -\frac{P_{i\nu}}{d_{i\nu}}(\bar{v}_\nu - \bar{v}_i) \quad \text{for all } (i, \nu) \in \mathcal{E}. \quad (6)$$

Hence, for each $i \in \mathcal{V}$ pick $j^*, k^* \in \mathcal{O}_i$ such that β_{ij^*} and β_{ik^*} are linearly independent. We now prove that there exists $\bar{\omega}_i \in \mathbb{R}^3$ such that (6) holds for $\nu = j^*$ and for $\nu = k^*$ which, due to Lemma 1 (see Appendix A.1), is equivalent to

$$\left(S(\beta_{ij^*})\frac{P_{ij^*}}{d_{ij^*}}(\bar{v}_{j^*} - \bar{v}_i) - S(\beta_{ik^*})\frac{P_{ik^*}}{d_{ik^*}}(\bar{v}_{k^*} - \bar{v}_i) \right)^\top (S(\beta_{ij^*})\beta_{ik^*}) = 0. \quad (7)$$

It can be shown that indeed (7) holds by using Binet-Cauchy's identity¹, and the hypothesis $A_{ij^*k^*}\bar{\mathbf{v}} = 0$ (see (3)).

Now, we show that $\bar{\omega}_i$ in fact satisfies (6) for all (i, l) such that $l \in \mathcal{O}_i$. From the non-degeneracy assumption, if $|\mathcal{O}_i| \geq 3$ there exists $l^* \in \mathcal{O}_i$ such that $\{\beta_{ij^*}, \beta_{ik^*}, \beta_{il^*}\}$ is linearly independent. Also,

$$\beta_{i\nu}^\top \left(\frac{P_{il^*}}{d_{il^*}}(\bar{v}_{l^*} - \bar{v}_i) + S(\beta_{il^*})\bar{\omega}_i \right) = 0, \quad \nu \in \{j^*, k^*, l^*\}.$$

When $\nu = l^*$, this holds trivially; when $\nu \in \{j^*, k^*\}$, this follows from $A_{ij^*l^*}\bar{\mathbf{v}} = A_{ik^*l^*}\bar{\mathbf{v}} = 0$ (see (3)) and (6). For the remaining $m \in \mathcal{O}_i \setminus \{j^*, k^*, l^*\}$, repeat the

¹Binet-Cauchy: $(S(x)y)^\top (S(v)w) = (x^\top v)(y^\top w) - (x^\top w)(y^\top v)$ for $x, y, v, w \in \mathbb{R}^3$.

process. Then, (6) follows for all $i \in \mathcal{V}$. Finally, since $\bar{\mathbf{v}} \notin \mathcal{T}_a$, it follows that $[\bar{\mathbf{v}}; \bar{\omega}] \notin \mathcal{T}_b$.

Necessity: we proceed with the following strategy. By assuming that $(\mathcal{G}, (\mathbf{p}, \mathbf{R}))$ is not IBR and that $\dim(\mathcal{B}_i) \geq d - 1 = 2$ for all $i \in \mathcal{V}$, we show that $(\mathcal{G}, \mathbf{p})$ is not IAR. Consider $[\bar{\mathbf{v}}; \bar{\omega}] \notin \mathcal{T}_b(\mathbf{p}, \mathbf{R})$ such that $B_{\mathcal{G}}(\mathbf{p}, \mathbf{R})[\bar{\mathbf{v}}; \bar{\omega}] = 0$. Thus, (6) holds. Also, for $(i, j, k) \in \mathcal{A}$,

$$\begin{aligned} A_{ijk}(\mathbf{p})\bar{\mathbf{v}} &= \beta_{ik}^\top \frac{P_{ij}}{d_{ij}}(\bar{v}_j - \bar{v}_i) + \beta_{ij}^\top \frac{P_{ik}}{d_{ik}}(\bar{v}_k - \bar{v}_i) \\ &= -(\beta_{ik}^\top S(\beta_{ij}) + \beta_{ij}^\top S(\beta_{ik}))\bar{\omega}_i = 0. \end{aligned}$$

We conclude that $A_{\mathcal{G}}(\mathbf{p})\bar{\mathbf{v}} = 0$. Finally, we show that $\bar{\mathbf{v}} \notin \mathcal{T}_a(\mathbf{p})$, for if $\bar{\mathbf{v}} \in \mathcal{T}_a(\mathbf{p})$, then from (4) there would exist $\omega \in \mathbb{R}^3$ such that $\bar{v}_j - \bar{v}_i = (\kappa \mathbf{I}_d + S(\omega))p_{ij}$. Then, noting that $P_{ij}S(p_{ij}) = S(p_{ij})$ yields

$$P_{ij}(\bar{v}_j - \bar{v}_i) = -S(p_{ij})\omega, \quad \text{for all } (i, j) \in \mathcal{E}. \quad (8)$$

Also, since $B_{\mathcal{G}}(\mathbf{p}, \mathbf{R})[\bar{\mathbf{v}}; \bar{\omega}] = 0$, it follows from (1) that

$$P_{ij}(\bar{v}_j - \bar{v}_i) = -S(p_{ij})\bar{\omega}_i, \quad \text{for all } (i, j) \in \mathcal{E}. \quad (9)$$

For all $i \in \mathcal{V}$, (8) and (9) imply $S(p_{ij})\bar{\omega}_i = S(p_{ij})\omega$ for each $j \in \mathcal{O}_i$. Thus, since $\dim(\mathcal{B}_i) \geq 2$, it follows that $\bar{\omega}_i = \omega$. This implies $[\bar{\mathbf{v}}; \bar{\omega}] \in \mathcal{T}_b$, a contradiction; hence, $\bar{\mathbf{v}} \notin \mathcal{T}_a$ and the claim follows. \square

4 Angle-based Estimation and Control

In this section, we first propose an angle-based localization algorithm and show its local exponential stability under switching topologies, provided that all visited graphs are infinitesimally rigid. Then, to ensure the convergence of this estimator during a prescribed mission, we develop a decentralized gradient-based controller aimed at maintaining an appropriate level of angle rigidity despite changes in the sensing topology while driving the robots to fulfill the mission.

4.1 The angle rigidity eigenvalue

Although Definition 2 characterizes infinitesimal rigidity, it fails to provide a measure of how rigid a framework is. To address this, we define the *symmetric angle rigidity matrix* as $\mathbf{A}_{\mathcal{G}}(\mathbf{p}) := A_{\mathcal{G}}(\mathbf{p})^\top A_{\mathcal{G}}(\mathbf{p})$. It follows that $(\mathcal{G}, \mathbf{p})$ is IAR if and only if the *angle rigidity eigenvalue* is strictly positive, that is,

$$\lambda_{d+d'+2}(\mathbf{A}_{\mathcal{G}}(\mathbf{p})) > 0, \quad (10)$$

where λ_k denotes the k -th smallest eigenvalue of $\mathbf{A}_{\mathcal{G}}(\mathbf{p})$. For convenience, we will omit the subscript and denote the rigidity eigenvalue simply by λ . We propose using it as an indicator of a framework's degree of rigidity, as has been done in the context of distance and bearing-based rigidity maintenance control [30, 25]. The rigidity eigenvalue not only characterizes infinitesimal rigidity, but is also crucial for evaluating both the convergence rate and the robustness to measurement noise

of angle-based estimators. See [18] for a comprehensive analysis of how the eigenvalues of matrices arising in angle-based localization influence the overall performance. Therefore, the main objective of rigidity maintenance control is to keep this eigenvalue as large as possible.

4.2 Angle-based Position Estimation

To estimate agents' positions from angle measurements, we adapt the approach for formation control proposed in [12] to the context of network localization and study its convergence under time-varying topologies. The goal for each agent is to distributedly obtain $\hat{p}_i \in \mathbb{R}^d$, an estimate of its position with respect to some (unknown) common reference frame. It is clear that the configuration scale cannot be retrieved from angles alone; hence, we assume that one robot can measure the distance to a neighbor. Let $\iota, \kappa \in \mathcal{V}$ such that $d_{\iota\kappa}$ is measured by ι .

Consider a finite family of graphs $\{\mathcal{G}_1, \dots, \mathcal{G}_M\}$ and a fixed collision-free configuration $\mathbf{p} \in \mathbb{R}^{d|\mathcal{V}|}$. Let $s : \mathbb{R}_{\geq 0} \rightarrow \{1, \dots, M\}$ be a piecewise-constant switching signal. We propose the following family of potential functions indexed by m ,

$$\mathcal{L}_m(\hat{\mathbf{p}}) := \frac{\gamma_a}{2} \|\alpha_{\mathcal{G}_m}(\hat{\mathbf{p}}) - \alpha_{\mathcal{G}_m}(\hat{\mathbf{p}})\|^2 + \frac{\gamma_s}{4} (\hat{d}_{\iota\kappa}^2 - d_{\iota\kappa}^2)^2, \quad (11)$$

where $\gamma_a, \gamma_s > 0$ and $\hat{d}_{\iota\kappa} := \|\hat{p}_\kappa - \hat{p}_\iota\|$ denotes the estimated distance. The proposed estimator is designed as the negative gradient of (11), $\dot{\hat{\mathbf{p}}}(t) = -\nabla_{\hat{\mathbf{p}}} \mathcal{L}_{s(t)}(\hat{\mathbf{p}}(t))$. For robot i , and omitting the dependence on m ,

$$\begin{aligned} \dot{\hat{p}}_i &= \gamma_a \sum_{\{j,k\} \subseteq \mathcal{O}_i} (\hat{\alpha}_{ijk} - \alpha_{ijk}) (\hat{\eta}_{ijk} + \hat{\eta}_{ikj}) - \\ &\gamma_a \sum_{\{i,k\} \subseteq \mathcal{O}_j} (\hat{\alpha}_{jik} - \alpha_{jik}) \hat{\eta}_{jik} - \\ &\gamma_s (\delta_{i\iota} - \delta_{i\kappa}) (\hat{d}_{\iota\kappa}^2 - d_{\iota\kappa}^2) (\hat{p}_\iota - \hat{p}_\kappa), \end{aligned} \quad (12)$$

where $\eta_{ijk} := P_{ij}\beta_{ik}/d_{ij}$ and δ_{ij} is Kronecker's delta. Here, \hat{x} indicates that variable x is computed using the estimated positions. To compute (12) in a decentralized manner, robot i requires: (a) for each $\{j, k\} \subseteq \mathcal{O}_i$, measure α_{ijk} and receive \hat{p}_j and \hat{p}_k ; (b) for each j, k such that $\{i, k\} \subseteq \mathcal{O}_j$, receive $(\hat{\alpha}_{jik} - \alpha_{jik})\hat{\eta}_{jik}$, which can be computed by j .

The following Proposition studies the convergence properties of (12).

Proposition 4 *Assume that \mathbf{p} is fixed and that $s(t)$ has finitely many discontinuities on every bounded interval. Moreover, assume that each $(\mathcal{G}_m, \mathbf{p}), m = 1, \dots, M$ is infinitesimally angle rigid. Then, under (12), the desired set*

$$\mathcal{S}(\mathbf{p}) := \{\mathbf{q} : \mathbf{q} = [Q\mathbf{p}_i + r]_{i \in \mathcal{V}}, (r, Q) \in \text{SE}(d)\}$$

is locally exponentially stable.

Proof. Since $\mathcal{S}(\mathbf{p})$ is a smooth embedded submanifold of $\mathbb{R}^{d|\mathcal{V}|}$, it has a tubular neighborhood \mathcal{U} for which

there is a smooth orthogonal projection, see [15]. Indeed, let $\Pi : \mathcal{U} \rightarrow \mathcal{S}(\mathbf{p})$ be such projection, then for each $\hat{\mathbf{p}} \in \mathcal{U}$, it holds that $\delta := \hat{\mathbf{p}} - \Pi(\hat{\mathbf{p}}) \in N_{\Pi(\hat{\mathbf{p}})}\mathcal{S}(\mathbf{p})$. Define

$$\mathcal{W}(\hat{\mathbf{p}}) := \frac{1}{2} \text{dist}(\hat{\mathbf{p}}, \mathcal{S}) = \frac{1}{2} \|\delta\|^2$$

as the Lyapunov function for the proposed estimator. Now, let $\hat{\mathbf{q}} := \Pi(\hat{\mathbf{p}})$, it follows that $\dot{\hat{\mathbf{q}}} \in T_{\hat{\mathbf{q}}}\mathcal{S}(\mathbf{p})$. Since $\delta \in N_{\hat{\mathbf{q}}}\mathcal{S}(\mathbf{p})$,

$$\dot{\mathcal{W}}(\hat{\mathbf{p}}) = \delta^\top \dot{\delta} = \delta^\top \dot{\hat{\mathbf{p}}} = -\delta^\top \nabla_{\hat{\mathbf{p}}} \mathcal{L}_m(\hat{\mathbf{p}}).$$

Now, we study the behavior of $\nabla_{\hat{\mathbf{p}}} \mathcal{L}_m$ near $\mathcal{S}(\mathbf{p})$. Since $\nabla_{\hat{\mathbf{p}}} \mathcal{L}_m(\hat{\mathbf{q}}) = 0$, its Taylor expansion near $\hat{\mathbf{q}}$ is

$$\nabla_{\hat{\mathbf{p}}} \mathcal{L}_m(\hat{\mathbf{p}}) = \nabla_{\hat{\mathbf{p}}} \mathcal{L}_m(\hat{\mathbf{q}} + \delta) = \nabla_{\hat{\mathbf{p}}}^2 \mathcal{L}_m(\hat{\mathbf{q}}) \delta + \varepsilon_m(\hat{\mathbf{q}}, \delta) \|\delta\|,$$

where $\|\varepsilon_m(\hat{\mathbf{q}}, \delta)\| \rightarrow 0$ as $\delta \rightarrow 0$.

On the other hand, for each $\mathbf{q} \in \mathcal{S}(\mathbf{p})$, the Hessian is

$$\nabla_{\hat{\mathbf{p}}}^2 \mathcal{L}_m(\mathbf{q}) = \gamma_a \mathbf{A}_{\mathcal{G}_m}(\mathbf{q}) + \gamma_s \mathbf{D}_{\iota\kappa}(\mathbf{q}), \quad (13)$$

where $\mathbf{A}_{\mathcal{G}_m}$ is the symmetric rigidity matrix and $\mathbf{D}_{\iota\kappa} := 2(e_\iota - e_\kappa)(e_\iota - e_\kappa)^\top \otimes q_{\iota\kappa} q_{\iota\kappa}^\top$, both positive semidefinite. From the infinitesimal rigidity assumption of \mathcal{G}_m it follows that $\text{Null}(\mathbf{A}_{\mathcal{G}_m}(\mathbf{q})) = T_{\mathbf{q}}\mathcal{S}(\mathbf{p}) + \text{span}\{\mathbf{q}\}$, the last term corresponding to configuration scalings, ruled out by including the term associated with $\mathbf{D}_{\iota\kappa}(\mathbf{q})$. It follows that, $\text{Null}(\mathbf{A}_{\mathcal{G}_m}) \cap \text{Null}(\mathbf{D}_{\iota\kappa}) = T_{\mathbf{q}}\mathcal{S}(\mathbf{p})$; hence, the Hessian (13) is positive definite on $N_{\mathbf{q}}\mathcal{S}(\mathbf{p})$. In particular, there is a lower bound $c > 0$ such that for all $m = 1, \dots, M$,

$$\mathbf{v}^\top \nabla_{\hat{\mathbf{p}}}^2 \mathcal{L}_m(\mathbf{q}) \mathbf{v} \geq c \|\mathbf{v}\|^2 \quad \text{for all } \mathbf{v} \in N_{\mathbf{q}}\mathcal{S}(\mathbf{p}). \quad (14)$$

Note that (14) holds uniformly in \mathbf{q} , since the spectrum of both $\mathbf{A}_{\mathcal{G}_m}$ and $\mathbf{D}_{\iota\kappa}$ is invariant along $\mathbf{q} \in \mathcal{S}(\mathbf{p})$. Finally, in a sufficiently small neighborhood,

$$\begin{aligned} \dot{\mathcal{W}}(\hat{\mathbf{p}}) &= -\delta^\top \nabla_{\hat{\mathbf{p}}}^2 \mathcal{L}_m(\hat{\mathbf{q}}) \delta - \delta^\top \varepsilon_m(\hat{\mathbf{q}}, \delta) \|\delta\| \\ &\leq (-c + \|\varepsilon_m(\hat{\mathbf{q}}, \delta)\|) \|\delta\|^2 \leq -\tilde{c} \|\delta\|^2 = -2\tilde{c} \mathcal{W}(\hat{\mathbf{p}}) \end{aligned}$$

for some $\tilde{c} > 0$. Here, we used $-\delta^\top \varepsilon_m(\hat{\mathbf{q}}, \delta) \leq \|\delta\| \|\varepsilon_m(\hat{\mathbf{q}}, \delta)\|$. Since \mathcal{W} is continuous and does not depend on m , one gets

$$\mathcal{W}(\hat{\mathbf{p}}(t)) \leq e^{-2\tilde{c}(t-t_0)} \mathcal{W}(\hat{\mathbf{p}}(t_0)),$$

and the claim follows. \square

Remark 1 *The use of angle measurements effectively decouples the estimation of the agents' positions from their orientations. This is important because in bearing-based localization, the position and orientation estimators are inherently coupled. As a result, the propagation of noisy orientation errors not only complicates the analysis of the position estimator but may also compromise its convergence.*

4.3 Decentralized Rigidity Maintenance Control

4.3.1 Robot model

We consider a team of robots moving in \mathbb{R}^d with single-integrator dynamics,

$$\dot{p}_i = R_i u_i^i, \quad \dot{R}_i = R_i S(\omega_i^i), \quad i \in \mathcal{V}, \quad (15)$$

where u_i^i and ω_i^i denote the control inputs, corresponding to linear and angular velocity in the body-frame, respectively. They are defined as

$$\begin{aligned} u_i^i &:= \gamma_r u_{i,r}^i + \gamma_c u_{i,c}^i + \gamma_m u_{i,m}^i, \\ \omega_i^i &:= \gamma'_r \omega_{i,r}^i + \gamma'_m \omega_{i,m}^i, \end{aligned} \quad (16)$$

where $\gamma_r, \gamma_c, \gamma_m, \gamma'_r, \gamma'_m > 0$ and each term corresponds to three objectives: rigidity maintenance (Section 4.3.3), collision avoidance (Section 4.4), and mission completion (Section 5.1).

In order to encode sensing constraints into the system's model, let the camera's optical axis be oriented towards the body-frame x -axis and represented by $R_i e_1$. Also, define $\zeta_{ij} := \beta_{ij}^\top R_i e_1 = (\beta_{ij}^i)^\top e_1$. Then, the sensing graph is determined by the edge set

$$\mathcal{E}(\mathbf{p}, \mathbf{R}) = \{(i, j) \in \mathcal{V} \times \mathcal{V} : d_{ij} < \rho_r, \zeta_{ij} > \rho_f\}, \quad (17)$$

where $\rho_r > 0$ and $\rho_f := \cos(\phi/2)$ with $0 \leq \phi < 2\pi$ are fixed and characterize the cameras' range and field of view, respectively. Note that, with this model, the angle set \mathcal{A} also depends on the joint pose (\mathbf{p}, \mathbf{R}) .

4.3.2 The weighted angle rigidity eigenvalue

Note that changes in the sensing topology introduce discontinuities in the rigidity eigenvalue (10). Therefore, due to (17), λ depends non-smoothly on (\mathbf{p}, \mathbf{R}) , which prevents its direct use in gradient-based controllers. To address this, we propose an approximation that *smoothly* accounts for the sensing constraints. We do this by assigning pose-dependent weights to each angle in \mathcal{A} . These weights are incorporated into the scheme via the *weighted* symmetric angle rigidity matrix

$$\tilde{\mathbf{A}}(\mathbf{p}, \mathbf{R}) := A_{\mathcal{G}}(\mathbf{p})^\top W(\mathbf{p}, \mathbf{R}) A_{\mathcal{G}}(\mathbf{p}), \quad (18)$$

where $\mathcal{G} = \mathcal{G}(\mathbf{p}, \mathbf{R})$, and $W \in \mathbb{R}^{|\mathcal{A}| \times |\mathcal{A}|}$ is a diagonal matrix that collects all the weights. The corresponding *weighted* rigidity eigenvalue is denoted by $\tilde{\lambda}(\mathbf{p}, \mathbf{R})$.

Weights are defined as follows. Let $w_{ijk} \in \mathbb{R}$ be the weight associated with $(i, j, k) \in \mathcal{A}$. Similar to [25, Section III.D], we employ the family $\sigma : \mathbb{R} \rightarrow [0, 1]$ of functions parameterized by $a, b \in \mathbb{R}$ defined as

$$\sigma(x; a, b) = \begin{cases} 0, & x < a \\ \frac{1}{2} \left(1 - \cos \left(\pi \frac{x-a}{b-a} \right) \right), & a \leq x \leq b \\ 1, & b < x \end{cases} \quad (19)$$

Hence, $\sigma(x; a, b)$ transitions (with a continuous derivative) from 0 to 1 as x varies from a to b . Let $\sigma_r(x) := \sigma(x; a_r, b_r)$ with $0 \leq a_r < b_r \leq \rho_r$ and define the weight $w_{r_{ij}} := 1 - \sigma_r(d_{ij})$ associated with edge (i, j) , which accounts for the limited sensing range. It follows that $w_{r_{ij}} = 1$ when $d_{ij} < a_r$ and smoothly approaches 0 as d_{ij} increases to b_r . Likewise, $\sigma_f(x) := \sigma(x; a_f, b_f)$ with $\rho_f \leq a_f < b_f \leq 1$ and $w_{f_{ij}} := \sigma_f(\zeta_{ij})$, which considers the limited field of view. Hence, $w_{f_{ij}} = 1$ when $\zeta_{ij} > b_f$ and smoothly approaches 0 as ζ_{ij} decreases to a_f . Analogously, define $w_{r_{ik}}$ and $w_{f_{ik}}$ for edge (i, k) . Finally, we set

$$w_{ijk} = d_{ij} d_{ik} w_{r_{ij}} w_{f_{ij}} w_{r_{ik}} w_{f_{ik}}. \quad (20)$$

Thus, $w_{ijk} > 0$ if and only if agents j and k are both captured by i 's camera, and w_{ijk} smoothly approaches 0 as any of them moves outside of it. The reason to include the factor $d_{ij} d_{ik}$ is to make $\tilde{\mathbf{A}}$ (and therefore $\tilde{\lambda}$) scale invariant. By checking (3), it follows that the symmetric rigidity matrix $\mathbf{A}_{\mathcal{G}}$ (and therefore λ) depends inversely on the square of the configuration scale. This implies that following the gradient of the rigidity eigenvalue drives the robots to collapse into a single point, which is undesirable.

Proposition 5 *If all weights are defined by (20), then in the open set where no robot collisions occur, $\tilde{\mathbf{A}}$ (18) is continuously differentiable with respect to (\mathbf{p}, \mathbf{R}) .*

Proof. First,

$$\tilde{\mathbf{A}}(\mathbf{p}, \mathbf{R}) = \sum_{(i,j,k) \in \mathcal{A}} w_{ijk} A_{ijk}^\top A_{ijk}.$$

The claim follows since all quantities involved are continuously differentiable with respect to (\mathbf{p}, \mathbf{R}) under the non-collision assumption, and from the fact that w_{ijk} smoothly approaches 0 as (i, j, k) is removed from \mathcal{A} . \square

4.3.3 Rigidity control action

As discussed, angle rigidity maintenance aims to prevent the rigidity eigenvalue from approaching zero. To this end, we propose the minimization of the following potential

$$\mathcal{R}(\mathbf{p}, \mathbf{R}) := -\log \left(\tilde{\lambda}(\mathbf{p}, \mathbf{R}) \right). \quad (21)$$

It is important to emphasize that the objective of angle rigidity maintenance fundamentally differs from angle-based formation or shape control. The potential (21) does not aim to enforce convergence to a prescribed set of angles or to maintain a fixed geometric shape. Instead, its sole purpose is to prevent the system from evolving toward configurations where the angle rigidity matrix loses rank. As a result, the angle set (and their values) is not required to remain constant along the trajectory, nor is the formation constrained to move rigidly as a whole.

Now, we obtain expressions for the body-frame rigidity control actions for agent i . Let $\tilde{\mathbf{v}} = [\tilde{v}_i]_{i \in \mathcal{V}}$ be a unit-norm eigenvector associated with $\tilde{\lambda}$. First, we express the weighted rigidity eigenvalue as a sum over all angles,

$$\tilde{\lambda}(\mathbf{p}, \mathbf{R}) = \tilde{\mathbf{v}}^\top \tilde{\mathbf{A}} \tilde{\mathbf{v}} = \sum_{(i,j,k) \in \mathcal{A}} w_{ijk} (A_{ijk} \tilde{\mathbf{v}})^2, \quad (22)$$

with $A_{ijk} \tilde{\mathbf{v}}$ as in (3). The gradient of (22) with respect to (p_i, R_i) is

$$\begin{aligned} \nabla_{p_i} \tilde{\lambda} &= \sum_{(\iota, \kappa, \ell) \in \mathcal{A}} \left((A_{\iota\kappa\ell} \tilde{\mathbf{v}})^2 \nabla_{p_i} w_{\iota\kappa\ell} + \right. \\ &\quad \left. 2w_{\iota\kappa\ell} (A_{\iota\kappa\ell} \tilde{\mathbf{v}}) \frac{\partial A_{\iota\kappa\ell}}{\partial p_i} \tilde{\mathbf{v}} \right), \\ \nabla_{R_i} \tilde{\lambda} &= \sum_{(\iota, \kappa, \ell) \in \mathcal{A}} (A_{\iota\kappa\ell} \tilde{\mathbf{v}})^2 \nabla_{R_i} w_{\iota\kappa\ell}. \end{aligned} \quad (23)$$

Remark 2 To obtain (23), we used $\frac{\partial \tilde{\lambda}}{\partial \xi} = \tilde{\mathbf{v}}^\top \frac{\partial \tilde{\mathbf{A}}}{\partial \xi} \tilde{\mathbf{v}}$, for each parameter $\xi \in \mathbb{R}$. This expression assumes that the rigidity eigenvalue has multiplicity one since, otherwise, $\tilde{\mathbf{v}}$ is not unique. Potential workarounds when $\tilde{\lambda}$ is not simple are discussed in [25, Section III.D] and [22, Section IV.B]. However, decentralized and scalable solutions for this problem are still a subject of research.

Finally, since terms in (23) vanish when $i \notin \{\iota, \kappa, \ell\}$,

$$\begin{aligned} w_{i,r}^i &:= -R_i^\top \nabla_{p_i} \mathcal{R} = \tilde{\lambda}^{-1} R_i^\top \nabla_{p_i} \tilde{\lambda} \\ &= \tilde{\lambda}^{-1} \sum_{\{j,k\} \subseteq \mathcal{O}_i} \left((A_{ijk} \tilde{\mathbf{v}})^2 (R_i^\top \nabla_{p_i} w_{ijk}) \right. \\ &\quad \left. + 2w_{ijk} (A_{ijk} \tilde{\mathbf{v}}) \left(R_i^\top \frac{\partial A_{ijk}}{\partial p_i} \tilde{\mathbf{v}} \right) \right) \end{aligned} \quad (24)$$

$$\begin{aligned} &+ \tilde{\lambda}^{-1} \sum_{\{i,k\} \subseteq \mathcal{O}_j} \left((A_{jik} \tilde{\mathbf{v}})^2 R_{ij} (R_j^\top \nabla_{p_i} w_{jik}) \right. \\ &\quad \left. + 2w_{jik} (A_{jik} \tilde{\mathbf{v}}) R_{ij} \left(R_j^\top \frac{\partial A_{jik}}{\partial p_i} \tilde{\mathbf{v}} \right) \right). \end{aligned}$$

$$\begin{aligned} \omega_{i,r}^i &:= -S^{-1} (R_i^\top \nabla_{R_i} \mathcal{R}) = \tilde{\lambda}^{-1} S^{-1} (R_i^\top \nabla_{R_i} \tilde{\lambda}) \\ &= \tilde{\lambda}^{-1} \sum_{\{j,k\} \subseteq \mathcal{O}_i} (A_{ijk} \tilde{\mathbf{v}})^2 S^{-1} (R_i^\top \nabla_{R_i} w_{ijk}) \end{aligned} \quad (25)$$

Remark 3 Expression (24) involves relative rotation $R_{ij} := R_i^\top R_j$, which we assume to be available to j if $(j, i) \in \mathcal{E}$. This term arises from the need to express gradient contributions in the body reference frames. The control itself does not require orientations as part of the state, nor does it require communication of the relative rotations between neighbors. Moreover, no additional constraints on the sensing graph are imposed beyond those already required for angle rigidity.

Remark 4 The rigidity eigenvalue $\tilde{\lambda}$ and the body-frame eigenvector $\tilde{\mathbf{v}}$ are global variables. In the context of bearing and angle rigidity, as discussed in [25], it should be feasible for each robot to estimate $\tilde{\lambda}$ and $\tilde{\mathbf{v}}_i^i := R_i^\top \tilde{\mathbf{v}}$ in a decentralized manner, following the approach in [30, 26]. We assume that these variables are available and leave their estimation for future work.

In what follows, we provide formulas to compute (24) and (25) from onboard measurements and communications between neighbors. This requires, for each robot i : (a) for each $\{j, k\} \subseteq \mathcal{O}_i$, to measure $\beta_{ij}^i, \beta_{ik}^i, R_{ij}$, and R_{ik} , and to receive $\hat{p}_j, \hat{p}_k, \tilde{\mathbf{v}}_j^j$, and $\tilde{\mathbf{v}}_k^k$; (b) for each j, k such that $\{i, k\} \subseteq \mathcal{O}_j$, to receive the corresponding term in the second summation of (24), which can be computed by j .

First, weight w_{ijk} can be computed from the estimated values d_{ij} and d_{ik} , and from ζ_{ij} and ζ_{ik} , obtained from body-frame bearings. Also,

$$A_{ijk} \tilde{\mathbf{v}} = (\eta_{ijk}^i)^\top (R_{ij} \tilde{\mathbf{v}}_j^j - \tilde{\mathbf{v}}_i^i) + (\eta_{ikj}^i)^\top (R_{ik} \tilde{\mathbf{v}}_k^k - \tilde{\mathbf{v}}_i^i) \quad (26)$$

where $\eta_{ijk}^i := P_{ij}^i \beta_{ik}^i / d_{ij}$ and $\eta_{ikj}^i := P_{ik}^i \beta_{ij}^i / d_{ik}$.

Second, we specify the gradients of the weights expressed in the body frame. Let σ'_r and σ'_f be the deriva-

tives of σ_r and σ_f , respectively. Then,

$$\begin{aligned} R_i^\top \nabla_{p_i} w_{ijk} &= w_{ijk} \left(\left(\frac{\sigma'_r(d_{ij})}{w_{r_{ij}}} - \frac{1}{d_{ij}} \right) \beta_{ij}^i + \right. \\ &\quad \left. \left(\frac{\sigma'_r(d_{ik})}{w_{r_{ik}}} - \frac{1}{d_{ik}} \right) \beta_{ik}^i - \frac{\sigma'_f(\zeta_{ij})}{w_{f_{ij} d_{ij}}} P_{ij}^i e_1 - \frac{\sigma'_f(\zeta_{ik})}{w_{f_{ik} d_{ik}}} P_{ik}^i e_1 \right), \end{aligned} \quad (27)$$

$$\begin{aligned} R_i^\top \nabla_{R_i} w_{ijk} &= \\ w_{ijk} S \left(S(e_1) \left(\frac{\sigma'_f(\zeta_{ij})}{w_{f_{ij}}} \beta_{ij}^i + \frac{\sigma'_f(\zeta_{ik})}{w_{f_{ik}}} \beta_{ik}^i \right) \right), \end{aligned} \quad (28)$$

$$\begin{aligned} R_j^\top \nabla_{p_i} w_{jik} &= \\ w_{jik} \left(\left(\frac{1}{d_{ji}} - \frac{\sigma'_r(d_{ji})}{w_{r_{ji}}} \right) \beta_{ji}^j + \frac{\sigma'_f(\zeta_{ji})}{w_{f_{ji} d_{ji}}} P_{ji}^j e_1 \right). \end{aligned} \quad (29)$$

See Appendix A.2 for the derivation of the gradients on $\text{SO}(d)$ used in (28). It is worth noting that all denominators in (27)–(29) cancel with w_{ijk}, w_{jik} , ensuring that all the gradients are well defined. Equivalent expressions without denominators can be derived, but they are more cumbersome. Additionally, (27)–(28) and (29) can be computed by i and j , respectively, using locally available quantities.

Third, we specify the derivatives of $A_{ijk} \tilde{\mathbf{v}}$ and $A_{jik} \tilde{\mathbf{v}}$. Define, for each i, j, k , the matrices

$$D_{ijk}^i := \frac{P_{ij}^i \beta_{ik}^i (\beta_{ij}^i)^\top + \beta_{ij}^i (\beta_{ik}^i)^\top P_{ij}^i + ((\beta_{ij}^i)^\top \beta_{ik}^i) P_{ij}^i}{d_{ij}^2},$$

$$E_{ijk}^i := \frac{P_{ij}^i P_{ik}^i}{d_{ij} d_{ik}}.$$

Then,

$$\begin{aligned} R_i^\top \frac{\partial A_{ijk}}{\partial p_i} \tilde{\mathbf{v}} &= (D_{ijk}^i - E_{ikj}^i) (R_{ij} \tilde{\mathbf{v}}_j^j - \tilde{\mathbf{v}}_i^i) \\ &\quad + (D_{ikj}^i - E_{ijk}^i) (R_{ik} \tilde{\mathbf{v}}_k^k - \tilde{\mathbf{v}}_i^i) \end{aligned} \quad (30)$$

$$\begin{aligned} R_j^\top \frac{\partial A_{jik}}{\partial p_i} \tilde{\mathbf{v}} &= -D_{jik}^j (R_{ji} \tilde{\mathbf{v}}_i^i - \tilde{\mathbf{v}}_j^j) \\ &\quad + E_{jik}^j (R_{jk} \tilde{\mathbf{v}}_k^k - \tilde{\mathbf{v}}_j^j). \end{aligned} \quad (31)$$

4.4 Collision avoidance

It can be observed that the rigidity maintenance control action depends inversely on the distances from each robot i to its neighbors; see (26), (30), and (31). To ensure the well-posedness of the control action, we include a collision avoidance mechanism. Consider the potential function

$$\mathcal{C}(\mathbf{p}) := \sum_{i \in \mathcal{V}} \sum_{j \in \mathcal{O}_i} \left(\frac{d_{ij} - \rho_r}{d_{ij}} \right)^2. \quad (32)$$

Each term of this cost grows unbounded as $d_{ij} \rightarrow 0$ and vanishes (with a vanishing derivative) as $d_{ij} \rightarrow \rho_r$. The body-frame collision avoidance action is

$$\begin{aligned} u_{i,c}^i &:= -R_i^\top \nabla_{p_i} \mathcal{C} = 2\rho_r \sum_{j \in \mathcal{O}_i} \frac{d_{ij} - \rho_r}{d_{ij}^3} \beta_{ij}^i \\ &\quad - 2\rho_r \sum_{i \in \mathcal{O}_j} \frac{d_{ij} - \rho_r}{d_{ij}^3} R_{ij} \beta_{ji}^j, \end{aligned} \quad (33)$$

which requires receiving body-frame bearings for each j for which $i \in \mathcal{O}_j$.

5 Validation

5.1 Cooperative mission

To validate the proposed approach, a cooperative mission involving multiple target tracking is proposed. Each robot i is assigned to track a (potentially distinct) target τ_i . This is done because, in order to fulfill this objective, robots move and orient their cameras along distinct, time-varying directions. As a result, changes in the sensing topology are generated, challenging the rigidity condition and testing the capabilities of both the estimator and the controller. These moving targets may be either physical objects in motion or the output of an algorithm that controls the cameras' motion for environmental exploration and related tasks.

Hence, we employ (19) to define the potential

$$\mathcal{M}(\mathbf{p}, \mathbf{R}) := \sum_{i \in \mathcal{V}} \mu_r \sigma_r(d_{i\tau_i}) + \mu_f (1 - \sigma_f(\zeta_{i\tau_i})), \quad (34)$$

with $\mu_r, \mu_f > 0$. For this application, a suitable choice of constants is $\mu_r = 1.5$, $\mu_f = 1.0$, $\sigma_r(x) := \sigma(x; 0, \rho_t)$, $\sigma_f(x) := \sigma(x; -1, 1)$, where ρ_t can be interpreted as a tracking radius. The (negative) gradient flow of (34) attracts the robot i and orients its camera toward a designated moving target τ_i if $d_{i\tau_i} < \rho_t$. The mission-related control action for robot i results in

$$\begin{aligned} u_{i,m}^i &:= -R_i^\top \nabla_{p_i} \mathcal{M} = \mu_r \sigma_r'(d_{i\tau_i}) \beta_{i\tau_i}^i - \mu_f \sigma_f'(\zeta_{i\tau_i}) \frac{P_{i\tau_i}^i}{d_{i\tau_i}} e_1 \\ \omega_{i,m}^i &:= -S^{-1} (R_i^\top \nabla_{R_i} \mathcal{M}) = \mu_f \sigma_f'(\zeta_{i\tau_i}) S(e_1) \beta_{i\tau_i}^i, \end{aligned} \quad (35)$$

which requires only the body-frame bearing. We assume that the distance to the target $d_{i\tau_i}$ is provided by the underlying tracking algorithm, either by specifying it as a setpoint or by estimating it from the camera images. The implementation of this procedure is beyond the scope of this work. Also, the target tracking control action depends inversely on $d_{i\tau_i}$; therefore, a term corresponding to robot-target collision should be added to (32) and (33).

5.2 Simulation Results

To validate the proposed control scheme, we performed simulations aimed at evaluating its performance and robustness under challenging conditions. We employed $N = 5$ robots in \mathbb{R}^3 . At $t = 0$ s, the robots' positions were randomly generated within a cube of $(40\text{m})^3$ and centered at $[80\text{m}; 20\text{m}; 20\text{m}]$, see Fig. 2. The cameras' axes were oriented toward the barycenter of all positions to obtain a sufficiently dense sensing graph at initialization. The cameras' parameters were set to $\rho_r = 30\text{m}$ and $\rho_f = 0.5$ (corresponding to a $\phi = 120^\circ$ field-of-view angle). The weights were defined using the values $a_r = 0.8\rho_r$, $b_r = \rho_r$, $a_f = \rho_f$, and $b_f = 1.4\rho_f$. The gains of the controller (see (16) and (35)) were $\gamma_r = 5$, $\gamma_c = 1$, $\gamma_m = 25$, $\gamma_r' = 0.5$, $\gamma_m' = 2.5$, $\mu_r = 6$, and $\mu_f = 1$. For this setup, 3 targets were used, which were tracked by robots 1, $\{2, 4\}$ and $\{3, 5\}$, respectively; hence $\tau_2 = \tau_4$ and $\tau_3 = \tau_5$. They followed

predefined trajectories within the cube $[0\text{m}, 100\text{m}]^3$. Example videos can be found in [13].

It can be seen that at $t = 0$ s all robots are engaged in mutual sensing, ensuring infinitesimal angle rigidity. Once the system is deployed, each robot i immediately begins to move closer to and aim at its assigned target τ_i . Because of asymmetries in the spatial configuration, some robots will be able to point towards their targets sooner than others, thereby losing visual contact with the rest of the team. The remaining robots must then focus on preserving the necessary bearing measurements (and thus the angles) required to maintain angle rigidity, since the relative importance of \mathcal{R} eventually exceeds \mathcal{M} . In this example (Fig. 2), three robots (the maximum possible for $N = 5$) lose visual contact with the team and successfully focus on tracking. The remaining two will adjust their positions and camera orientations in order to maintain angle rigidity throughout the mission.

Fig. 3 presents performance metrics. Fig. 3a shows the evolution of the angle rigidity eigenvalue, including both weighted and unweighted versions. The latter was scaled using the distances $\{d_{ij}d_{ik} : (i, j, k) \in \mathcal{A}\}$ for appropriate comparison. It can be seen how the rigidity eigenvalue λ_8 was kept positive at all times, ensuring the system's infinitesimal angle rigidity. In addition, $\tilde{\lambda}_8 \leq \lambda_8$ and, although they start close to each other, their difference increases rapidly after $t \approx 40$ s, indicating that the robot configuration induces weights that are positive but small. This lets the controller know that some angle measurements are close to being lost. It is interesting to notice that λ_8 (which is the one that determines the performance of the angle-based estimators) remains approximately constant, despite the number of edges (bearing measurements) decreasing over time as the robots disperse. This demonstrates the controller's ability to compensate for the loss of bearing measurements by optimizing the robots' geometric configuration.

Fig. 3b displays how the targets are visually tracked by the robots as the mission progresses. It shows the angles between the camera axes Re_1 and the bearing vectors $\beta_{i\tau_i}$, i.e., $\arccos(\zeta_{i\tau_i})$. For target τ_i to be captured by robot i 's camera, the angle $\arccos(\zeta_{i\tau_i})$ must be smaller than half of the field of view (60°). Moreover, these angles decrease as the robot better aims at the target. Here, the lines that remain below 60° correspond to robots 1, 4, and 5; therefore, each target is successfully tracked by one agent. Figure 3c presents the position estimation error obtained by applying the localization scheme described in Section 4.2, where $\iota = 0$, $\kappa = 1$, $\gamma_a = 1000$ and $\gamma_s = 0.05$. For each robot i , the initial estimate \hat{p}_i was generated by sampling from a normal distribution with mean p_i and standard deviation 2 m. The errors show a sustained decrease as the mission progresses and remain below $\approx 0.5\text{m}$, demonstrating the effectiveness of the angle-based estimator despite time-varying conditions.

A second configuration was tested, using $N = 8$ robots and a single target. In this case, the target moves rapidly along a trajectory surrounding a sphere

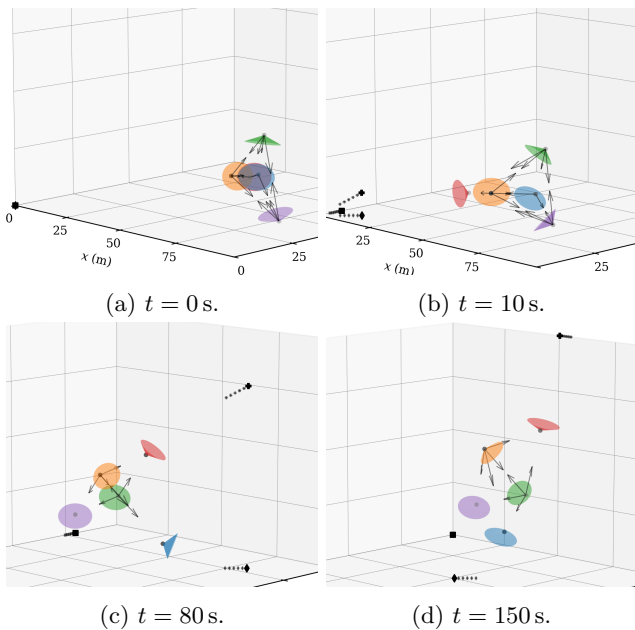


Figure 2: State of the system at different stages. Cameras are depicted as cones with apex located at p_i and aiming at $R_i e_1$. The field of view ϕ is drawn to scale, while the range ρ_r is not. Arrows represent acquired bearing measurements.

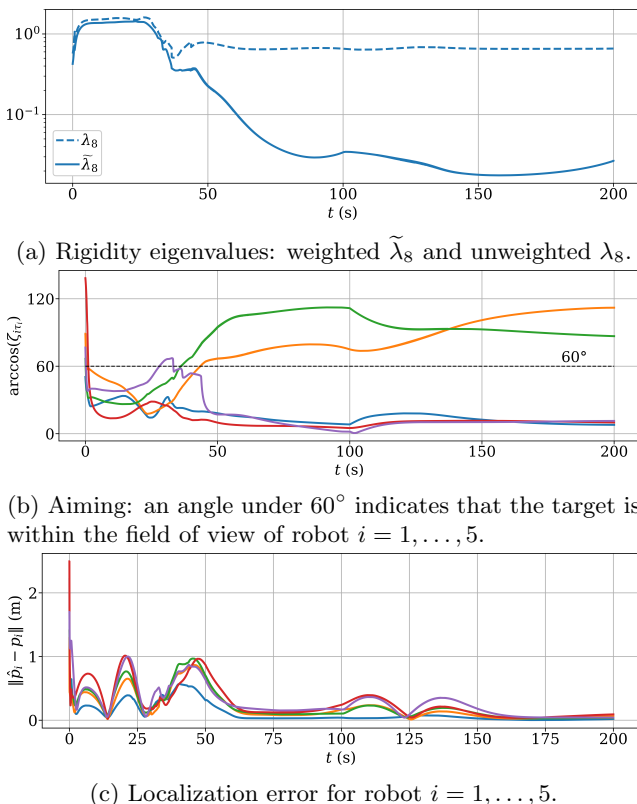
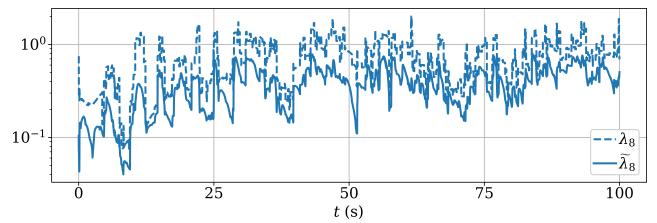
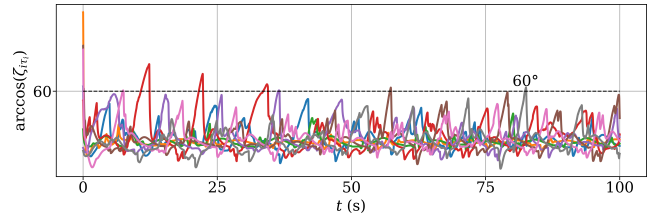


Figure 3: Control performance metrics.

that contains all the robots, inducing fast camera motions and frequent topology changes. The controller successfully handles this scenario while ensuring that the rigidity eigenvalue remains positive. Performance metrics are shown in Fig. 4 and example videos in [14].



(a) Rigidity eigenvalues: weighted $\tilde{\lambda}_8$ and unweighted λ_8 .



(b) Aiming: an angle under 60° indicates that the target is within the field of view of robot $i = 1, \dots, 5$.

Figure 4: Control performance metrics (second case).

6 Conclusions and Future Work

This work studied angle-based localization and decentralized rigidity maintenance control for multi-robot networks with sensing constraints. First, we provided a formal equivalence between bearing rigidity and angle rigidity that considers *directed* sensing graphs and *body-frame* bearing measurements in both 2 and 3-dimensional space. Subsequently, we proposed an angle-based localization protocol that only requires infinitesimal angle rigidity, and demonstrated its exponential convergence under time-varying topologies.

Additionally, the angle rigidity eigenvalue was proposed as a measure of a framework's degree of rigidity. Closed-form expressions for the rigidity eigenvalue and its gradient were derived. Subsequently, a decentralized rigidity maintenance controller was proposed and validated through simulations for the application of cooperative multi-target tracking. This demonstrated the controller's ability to handle multiple objectives and sensing constraints while avoiding collisions and maintaining a sufficient level of angle rigidity. This analysis revealed that, although relative rotations are not necessary for angle-based localization, they are required for rigidity maintenance, thus implying additional sensing capabilities. Nevertheless, angle-based approach remain advantageous since they decouple the position estimation from the robots' orientations (a) liberating some robots from mutual sensing; (b) eliminating the introduction of orientation errors into the estimator.

Future work will continue along the following directions. First, while the angle-based localization approach adopted here removes the need for orientation estimation, the relative rotations between robots are necessary for the computation of angle rigidity maintenance. Therefore, we plan to investigate the problem of estimating R_{ij} without introducing additional sensing assumptions. Second, in this work, we employed all the angles induced by a given set of bearing measurements. While theoretically sound, this approach may render some angles redundant, resulting in increased

computation and communication load. Therefore, it is of interest to study schemes for dynamically selecting suitable subsets of angles in a decentralized fashion.

References

- [1] P-A Absil, Robert Mahony, and Rodolphe Sepulchre. *Optimization algorithms on matrix manifolds*. Princeton University Press, 2008.
- [2] Mouaad Boughellaba and Abdelhamid Tayebi. Bearing-based distributed pose estimation for multi-agent networks. *IEEE Control Systems Letters*, 7:2617–2622, 2023.
- [3] Mouaad Boughellaba and Abdelhamid Tayebi. Distributed attitude estimation for multiagent systems on $so(3)$. *IEEE Transactions on Automatic Control*, 70(1):657–664, 2025.
- [4] Kun Cao, Zhimin Han, Zhiyun Lin, and Lihua Xie. Bearing-only distributed localization: A unified barycentric approach. *Automatica*, 133:109834, 2021.
- [5] Nicola De Carli, Paolo Salaris, and Paolo Robuffo Giordano. Multi-robot active sensing for bearing formations. In *2023 International Symposium on Multi-Robot and Multi-Agent Systems (MRS)*, pages 184–190, 2023.
- [6] Liangming Chen. Triangular angle rigidity for distributed localization in 2d. *Automatica*, 143:110414, 2022.
- [7] Liangming Chen, Kun Cao, Lihua Xie, Xiaolei Li, and Mir Feroskhan. 3-d network localization using angle measurements and reduced communication. *IEEE Transactions on Signal Processing*, 70:2402–2415, 2022.
- [8] Liangming Chen, Lihua Xie, Xiaolei Li, Xu Fang, and Mir Feroskhan. Simultaneous localization and formation using angle-only measurements in 2d. *Automatica*, 146:110605, 2022.
- [9] Leonardo Colombo, Hector Garcia de Marina, María Barbero Liñán, and David Martín de Diego. On the observability of relative positions in left-invariant multi-agent control systems and its application to formation control. In *2019 IEEE 58th Conference on Decision and Control (CDC)*, pages 7333–7338, 2019.
- [10] Jinpeng Huang and Gangshan Jing. On the equivalence between signed angle rigidity and bearing rigidity. In *2025 IEEE 64th Conference on Decision and Control (CDC)*, pages 5935–5940, 2025.
- [11] Gangshan Jing, Changhuang Wan, and Ran Dai. Angle-based sensor network localization. *IEEE Transactions on Automatic Control*, 67(2):840–855, 2021.
- [12] Gangshan Jing, Guofeng Zhang, Heung Wing Joseph Lee, and Long Wang. Angle-based shape determination theory of planar graphs with application to formation stabilization. *Automatica*, 105:117–129, 2019.
- [13] LAR-UBA and CAR-CSIC. Angle-based localization and rigidity maintenance control for multi-robot networks [simulation demo]. <https://youtu.be/p-fdysUBRKc>, 2026. Accessed: 2026-03-30.
- [14] LAR-UBA and CAR-CSIC. Angle-based localization and rigidity maintenance control for multi-robot networks [simulation demo]. https://youtu.be/ZeDnGq5eh_E, 2026. Accessed: 2026-03-30.
- [15] John M. Lee. *Introduction to Smooth Manifolds*, volume 218 of *Graduate Texts in Mathematics*. Springer, New York, 2 edition, 2013.
- [16] Spyridon Leonardos, Kostas Daniilidis, and Roberto Tron. Distributed 3-d bearing-only orientation localization. In *2019 IEEE 58th Conference on Decision and Control (CDC)*, pages 1834–1841, 2019.
- [17] Xiaolei Li, Xiaoyuan Luo, and Shiyu Zhao. Globally convergent distributed network localization using locally measured bearings. *IEEE Transactions on Control of Network Systems*, 7(1):245–253, 2020.
- [18] Chenyang Liang, Liangming Chen, Yibei Li, Jie Mei, and Lihua Xie. Performance optimization of angle-based network localization. In *2023 62nd IEEE Conference on Decision and Control (CDC)*, pages 5159–5164, 2023.
- [19] Giulia Michieletto, Angelo Cenedese, and Antonio Franchi. Bearing rigidity theory in $se(3)$. In *2016 IEEE 55th Conference on Decision and Control (CDC)*, pages 5950–5955, 2016.
- [20] Giulia Michieletto, Angelo Cenedese, and Daniel Zelazo. A unified dissertation on bearing rigidity theory. *IEEE Transactions on Control of Network Systems*, 8(4):1624–1636, 2021.
- [21] Giulia Piovan, Iman Shames, Barış Fidan, Francesco Bullo, and Brian DO Anderson. On frame and orientation localization for relative sensing networks. *Automatica*, 49(1):206–213, 2013.
- [22] J. Francisco Presenza, Ignacio Mas, J. Ignacio Alvarez-Hamelin, and Juan I. Giribet. Subframework-based bearing rigidity maintenance control in multirobot networks. *IEEE Control Systems Letters*, 9:1249–1254, 2025.
- [23] Juan F. Presenza, J. Ignacio Alvarez-Hamelin, Ignacio Mas, and Juan I. Giribet. Subframework-based rigidity control in multirobot networks. In *2022 American Control Conference (ACC)*, pages 3431–3436, 2022.

- [24] Fabrizio Schiano, Antonio Franchi, Daniel Zelazo, and Paolo Robuffo Giordano. A rigidity-based decentralized bearing formation controller for groups of quadrotor uavs. In *2016 IEEE/RSJ International Conference on Intelligent Robots and Systems (IROS)*, pages 5099–5106, 2016.
- [25] Fabrizio Schiano and Paolo Robuffo Giordano. Bearing rigidity maintenance for formations of quadrotor uavs. In *2017 IEEE International Conference on Robotics and Automation (ICRA)*, pages 1467–1474, 2017.
- [26] Zhiyong Sun, Changbin Yu, and Brian D. O. Anderson. Distributed optimization on proximity network rigidity via robotic movements. In *2015 34th Chinese Control Conference (CCC)*, pages 6954–6960, 2015.
- [27] Quoc Van Tran, Brian D.O. Anderson, and Hyo-Sung Ahn. Pose localization of leader–follower networks with direction measurements. *Automatica*, 120:109125, 2020.
- [28] Minh Hoang Trinh, Byung-Hun Lee, Mengbin Ye, and Hyo-Sung Ahn. Bearing-based formation control and network localization via global orientation estimation. In *2018 IEEE conference on control technology and applications (CCTA)*, pages 1084–1089. IEEE, 2018.
- [29] Quoc Van Tran, Hyo-Sung Ahn, and Brian DO Anderson. Distributed orientation localization of multi-agent systems in 3-dimensional space with direction-only measurements. In *2018 IEEE Conference on Decision and Control (CDC)*, pages 2883–2889. IEEE, 2018.
- [30] Daniel Zelazo, Antonio Franchi, Heinrich H. Bühlhoff, and Paolo Robuffo Giordano. Decentralized rigidity maintenance control with range measurements for multi-robot systems. *The International Journal of Robotics Research*, 34(1):105–128, 2015.
- [31] Daniel Zelazo, Antonio Franchi, and Paolo Robuffo Giordano. Rigidity theory in se (2) for unscaled relative position estimation using only bearing measurements. In *2014 European Control Conference (ECC)*, pages 2703–2708. IEEE, 2014.
- [32] Shiyu Zhao and Daniel Zelazo. Bearing rigidity theory and its applications for control and estimation of network systems: Life beyond distance rigidity. *IEEE Control Systems Magazine*, 39(2):66–83, 2019.

following system of linear equations where x is the unknown

$$S(z_1)x = y_1 \quad \text{and} \quad S(z_2)x = y_2.$$

The system has solution if and only if

$$S(z_1)y_1 - S(z_2)y_2 \perp S(z_1)z_2,$$

and that solution is unique.

Proof. First, observe that $-S(z_i)y_i$ is a particular solution of the respective sub-system, and that $\text{Null } S(z_i) = \alpha_i z_i$. Hence, the existence of a solution x^* is equivalent to the existence of $\alpha_1, \alpha_2 \in \mathbb{R}$ such that

$$-S(z_1)y_1 + \alpha_1 z_1 = -S(z_2)y_2 + \alpha_2 z_2 =: x^*.$$

The previous condition is also equivalent to

$$S(z_1)y_1 - S(z_2)y_2 \in \text{span}\{z_1, z_2\}.$$

Finally, due to the linear independence between z_1 and z_2 , this is equivalent to

$$S(z_1)y_1 - S(z_2)y_2 \perp S(z_1)z_2.$$

To see that the solution is unique, observe that x^* is the intersection point of two non-parallel ($z_1 \neq \pm z_2$) lines in \mathbb{R}^3 . \square

A.2 Gradient computation on $\text{SO}(d)$

Here we show how to compute the gradient of a quadratic function $f : \text{SO}(d) \rightarrow \mathbb{R}$, $f(R) = x^\top R y$, with respect to the Riemannian metric $\langle A, B \rangle := \frac{1}{2} \text{Tr}(A^\top B)$. This is a required step to obtain (28). To do that, consider

$$g : \mathbb{R}^{d \times d} \rightarrow \mathbb{R}, \quad g(A) = x^\top A y \implies \nabla_A g(A) = 2xy^\top.$$

Then,

$$\nabla_R f(R) = R \text{skew}(R^\top \nabla_A g(R))$$

where $\text{skew}(A) := \frac{1}{2}(A - A^\top)$, see [1]. Therefore,

$$R^\top \nabla_R (x^\top R y) = \text{skew}(R^\top 2xy^\top) = (R^\top xy^\top - yx^\top R).$$

A Appendix

A.1 A useful lemma

Lemma 1 *Let $x, y_1, y_2, z_1, z_2 \in \mathbb{R}^3$ such that $z_1 \neq \pm z_2$, $\|z_1\| = \|z_2\| = 1$, $z_1 \perp y_1$, $z_2 \perp y_2$. Consider the*